Cellular and Molecular Biology
E-ISSN : 1165-158X / P-ISSN : 0145-5680
www.cellmolbiol.org

Original Research

Radiation-induced graft polymerization of elastin onto polyvinylpyrrolidone as a possible wound dressing

María Luisa Del Prado-Audelo[1,2*], Francisco J. Gómez-Zaldivar[1], Mario Pérez-Díaz[3], Roberto Sánchez-Sánchez[3], Maykel González-Torres[4], Manuel González-Del Carmen[5], Gabriela Figueroa-González[6], Javad Sharifi-Rad[7,8], Octavio D. Reyes-Hernández[9], Hernán Cortés[10], Gerardo Leyva-Gómez[1*]

[1] Departamento de Farmacia, Facultad de Química, Universidad Nacional Autónoma de México, Circuito Exterior S/N, Del. Coyoacán, Mexico City, 04510, Mexico
[2] Escuela de Ingeniería y Ciencias, Departamento de Bioingeniería, Tecnológico de Monterrey Campus Ciudad de México, Ciudad de México, 14380, Mexico
[3] Unidad de Ingeniería de Tejidos, Terapia Celular y Medicina Regenerativa, Instituto Nacional de Rehabilitación Luis Guillermo Ibarra Ibarra, Calz. México Xochimilco No 289 Col. Arenal de Guadalupe, C.P.14389 Mexico City, Mexico
[4] CONACyT-Laboratorio de Biotecnología, Instituto Nacional de Rehabilitación Luis Guillermo Ibarra Ibarra, Ciudad de México 14389, Mexico
[5] Facultad de Medicina, Universidad Veracruzana, Mendoza 94740, Veracruz, Mexico
[6] Laboratorio de Farmacogenética, UMIEZ, Facultad de Estudios Superiores Zaragoza, Universidad Nacional Autónoma de México, Ciudad de México 09230, Mexico
[7] Phytochemistry Research Center, Shahid Beheshti University of Medical Sciences, Tehran, Iran
[8] Facultad de Medicina, Universidad del Azuay, Cuenca, Ecuador
[9] Laboratorio de Biología Molecular del Cáncer, UMIEZ, Facultad de Estudios Superiores Zaragoza, Universidad Nacional Autónoma de México, Ciudad de México 09230, Mexico
[10] Laboratorio de Medicina Genómica, Departamento de Genética, Centro Nacional de Investigación y Atención de Quemados (CENIAQ), Instituto Nacional de Rehabilitación-Luis Guillermo Ibarra Ibarra (INR-LGII), Ciudad de México, Mexico

[*]**Correspondence to:** luisa.delpradoa@gmail.com; leyva@quimica.unam.mx

Received August 7, 2020; **Accepted** November 4, 2020; **Published** January 31, 2021
Doi: http://dx.doi.org/10.14715/cmb/2021.67.1.10

Abstract: The purpose of our study was to obtain new wound dressings in the form of hydrogels that promote wound healing taking advantage of the broad activities of elastin (ELT) in physiological processes. The hydrogel of ELT and polyvinylpyrrolidone (PVP; ELT–PVP) was obtained by cross-linking induced by gamma irradiation at a dose of 25 kGy. The physicochemical changes attributed to cross-linking were analyzed through scanning electron microscopy (SEM), infrared spectroscopy analysis with Fourier transform (FTIR), differential scanning calorimetry (DSC), and thermogravimetric analysis (TGA). Furthermore, we performed a rheological study to determine the possible changes in the fluidic macroscopic properties produced by the cross-linking method. Finally, we accomplished viability and proliferation analyses of human dermal fibroblasts in the presence of the hydrogel to evaluate its biological characteristics. The hydrogel exhibited a porous morphology, showing interconnected porous with an average pore size of 16 ± 8.42 µm. The analysis of FTIR, DSC, and TGA revealed changes in the chemical structure of the ELT–PVP hydrogel after the irradiation process. Also, the hydrogel exhibited a rheological behavior of a pseudoplastic and thixotropic fluid. The hydrogel was biocompatible, demonstrating high cell viability, whereas ELT presented low biocompatibility at high concentrations. In summary, the hydrogel obtained by gamma irradiation revealed the appropriate morphology to be applied as a wound dressing. Interestingly, the hydrogel exhibited a higher percentage of cell viability compared with ELT, suggesting that the cross-linking of ELT with PVP is a suitable strategy for biological applications of ELT without generating cellular damage.

Key words: Wound dressing; Hydrogels; Elastin; Polyvinylpyrrolidone; Biopolymers.

Introduction

Skin lesions due to burns, pressure ulcers, or diabetes represent a global problem due to the exceptional management required. The significant fluid loss, tissue damage, and the probability of infection exemplify parameters to consider in wound healing. In this regard, the use of dressings as a treatment for wound healing signifies an attractive option because they promote an ideal micro-environment for recovery, preserve the moisture in the wound, provide adequate gas exchange, stimulate the synthesis of growth factors, and protect the wound from pathogens (1,2). In recent years, the use of wound dressings based on biopolymers has generated massive interest because they offer certain advantages over other materials (3–5), such as biocompatibility, high biodegradability, and the ability to stimulate the tissue regeneration (6). Moreover, these biopolymers can be combined with other synthetic polymers to form reinforced dressings such as hydrogels.

Hydrogels are three-dimensional networks characterized by their high hydrophilicity. These can be obtained by physical or chemical methods of poly-

mers cross-linking, such as gamma irradiation (7,8). Cross-linking by gamma irradiation is an efficient method for hydrogels synthesis (9) because the gamma rays possess the required energy to ionize molecules either in the air or in water (10), generating reactive sites along the polymer chain, allowing the combination of these radicals, and leading to the formation of a large number of cross-links (7). Besides, this chemical modification improves the physicochemical and mechanical properties of the combined biopolymers, while their natural biocompatibility, biodegradability, and lack of immunogenicity are retained.

In this respect, elastin (ELT) and polyvinylpyrrolidone (PVP) are polymers widely used for the manufacture of biomedical scaffolds (11). ELT is a structural protein of the extracellular matrix that provides elasticity and strength to various tissues (12). It also modulates cellular behavior, triggering biological responses such as chemotaxis, cell migration, and proliferation (13). Likewise, ELT is part of the architecture that supports cell growth, and its synthesis is involved in the production and maintenance of tissues. Due to these functions, ELT allows the formation of sophisticated biomaterials (14). On the other hand, the PVP is a biocompatible and biodegradable polymer that exhibits interesting biological properties, including low toxicity, the suitable transmission of water vapor, and impermeability to bacteria (8).

This study aimed to obtain a new polymer (ELT–PVP hydrogel) through the simultaneous irradiation of polymers in aqueous solution (15). The hydrogel was characterized through physicochemical and biological techniques to describe its novel chemical structure and biological compatibility as a potential activity for wound dressing in the repair of wounds. The hydrogel presented interconnected porous, which could permit cell internalization and migration during wound healing. It also showed a rheological profile of a pseudoplastic type due to the cross-linking of ELT and PVP. Regarding the biological activity, cell proliferation and viability tests were performed in human dermal fibroblasts, which revealed that the ELT–PVP hydrogel was biocompatible after the chemical cross-linking.

Materials and Methods

Materials

Alpha fraction hydrolyzed ELT (70,000 Da) was purchased from Drogueria Cosmopolita (Mexico City, Mexico), and PVP K-30 (8,000 Da) was obtained from BASF® (Ludwigshafen, Germany). Fetal bovine serum, penicillin, phosphate-buffered saline, and streptomycin were acquired from GIBCO® (United Kingdom). DMEM/F12 medium and viability/cytotoxicity kit for mammalian cells were obtained from ThermoFisher Scientific (Carlsbad, CA, USA). Crystal violet was purchased from ROTH® (Karlsruhe, Germany), and paraformaldehyde was acquired from Merck® (Germany).

Methods

Synthesis of ELT–PVP hydrogel

Alpha fraction hydrolyzed ELT was blended with PVP K-30 maintaining a 15:1 ratio of PVP to ELT (7.45% w/v and 0.5% w/v, respectively) to obtain a final concentration of 7.95% w/v. The mixture was irradiated at 25 kGy with ^{60}Co in a Gammabeam 651PT deep pool type radiator (Instituto de Ciencias Nucleares, Universidad Nacional Autónoma de México, Mexico City). For dosimetry, Fricke dosimeters, acrylics, and radiochromic dye films were used. ELT and copolymer (ELT–PVP) samples were lyophilized at conditions of -49 °C and 0.06 mBar for 24 h (FreeZone 1, Labconco®, MO, USA).

Scanning electron microscopy

In order to determine the morphology of the ELT–PVP hydrogel, the lyophilized sample was analyzed by scanning electron microscope (SEM; JCM6000, Jeol, Japan) under high vacuum conditions, and the pore size was determined using the ImageJ software**.**

Swelling ratio test

Dry and pre-weighed samples of ELT–PVP hydrogel were immersed into PBS 1X at room temperature to evaluate the absorption capacity. The excess of PBS was removed at different time intervals (0, 1, 2, 3, 4, 5, 6, and 7 days), and the weight of the samples was recorded. For each time, three samples were evaluated, and the results were expressed as mean ± SD. The percent of swelling ratio was calculated using the following formula:

$$\%\, swelling = \frac{W_f - W_i}{W_i} * 100$$

Where W_i refers to the weight of the dry sample, and W_f is the weight of the swollen sample.

Spectral analysis

Infrared spectroscopy analysis with Fourier transform (FTIR) was carried out to determine the functional groups present in the samples of the ELT–PVP hydrogel. The evaluation was performed through an infrared spectrometer (Alpha-FT-IR Bruker, USA), and measurements were made in a range of 400 to 4,000 cm^{-1}, with a resolution of 2 cm^{-1}.

Thermal properties

The thermogravimetric analysis (TGA) of the lyophilized samples was carried out in a calorimeter Q5000 (TA Instruments, Delaware, USA) to evaluate the thermal properties of the polymers. The analysis was carried out at a heating rate of 10 °C/min, with a temperature range of 0-800 °C, under a nitrogen atmosphere. The weight loss was determined from the experimental data. Differential scanning calorimetry (DSC) was performed on a calorimeter Q2000 (TA Instruments, Delaware, USA) at a heating rate of 10 °C/min, with a temperature range of 20-350 °C. Enthalpy changes were determined from the experimental data.

Rheology

In order to determine the viscosity profiles, the rheology analysis was performed in a viscometer (Brookfield CAP 2000 viscometer, USA), using the No.1 needle, with a constant temperature of 37 °C and controlled humidity. The shear rate experiment was performed from 1,600-8,000 s^{-1} and vice versa at intervals of 1,600 s^{-1}, the viscosity records were made after rotating for 20 s at each shear rate (16). Also, experiments at the constant shear rate were carried out at 2,000 s^{-1} during 1,800 s. The viscosity record was made every 120 s. Each sample was analyzed in triplicate using 250 µL of sample per analysis.

Cell viability assay

Calcein and ethidium homodimer (EthD-1) assays were carried out in human dermal fibroblasts to analyze the hydrogels cytotoxicity. Viability/cytotoxicity Kit for Mammalian Cells was used according to the manufacturer´s specifications. Fibroblasts were cultured with DMEM/F12 medium supplemented with 10% w/v of FBS and 1% w/v of penicillin/streptomycin. After 10th pass, 10,000 cells were cultured per well in 48 well culture plates and were treated with the following experimental conditions: PBS (control), ELT (0.1, 0.15, 0.2 and 0.25% w/v), or ELT–PVP (0.1, 0.15, 0.2 and 0.25% w/v). The concentration ratio of ELT–PVP was according to the concentration of ELT in the hydrogel. The cells were incubated with the treatments for 24 hours; then, they were stained with calcein (1 µM) and EthD-1 (2 µM) for one hour. Photographs were taken in an epifluorescent microscope (Zeiss Axiovert), and the number and percentage of positive cells for calcein and EthD-1 were counted using ImageJ software.

Cell proliferation assay

The analysis of the promotion of cell proliferation by the hydrogels was performed through a proliferation curve using crystal violet (CV) and human dermal fibroblasts. First, 2,500 fibroblasts were seeded in a 48 well culture plates and incubated with the following experimental conditions: PBS (control), ELT (0.15, 0.2 and 0.25% w/v), or ELT–PVP (0.1, 0.15, 0.2 and 0.25% w/v). The concentration ratio was according to the concentration of ELT in the hydrogel ELT–PVP. Each 24 h during three days, cells were fixed with paraformaldehyde 4% w/v, washed with PBS 1X, and then stained with 5% w/v of CV for 15 min. After, the cells were washed ten times with water, and the wells were dried with filter paper. Finally, 200 µL of methanol was added, and the optical density was measured at 570 nm in a plate reader (Synergy) to obtain the CV concentration. The results were compared with a standard curve to register the number of cells each day of the experiment.

Stability of ELT–PVP in cell culture medium

In order to analyze the ELT–PVP stability and degradation, the samples were immersed in DMEM medium supplemented with FBS, maintaining the culture conditions (37 ºC, 5% CO^2). Images of hydrogel were recorded at 1, 3, and 7 days of culture in a ZEISS Axio Zoom.V16 Microscope.

Results

Morphology of the ELT–PVP hydrogel

The morphology of the ELT–PVP hydrogel was examined by SEM; its microstructure is depicted in Figure 1. The new biopolymer presented an interconnected porous structure, where the average pore size was 16 ± 8.42 µm.

Swelling

The swelling behavior of ELT–PVP is showed in Figure 2. The highest percentage of the swelling ratio (40 %) was observed at 72 h of the experiment. Negative values indicated the dissolution process after reaching the water uptake equilibrium.

Spectral analysis

In order to analyze the possible chemical changes due to gamma radiation, FTIR was performed to ELT, PVP, ELT+PVP, and ELT–PVP (Figure 3). For ELT spectrum (line a), the signal of 1,646 cm^{-1} corresponded to the amide I band, while the bands

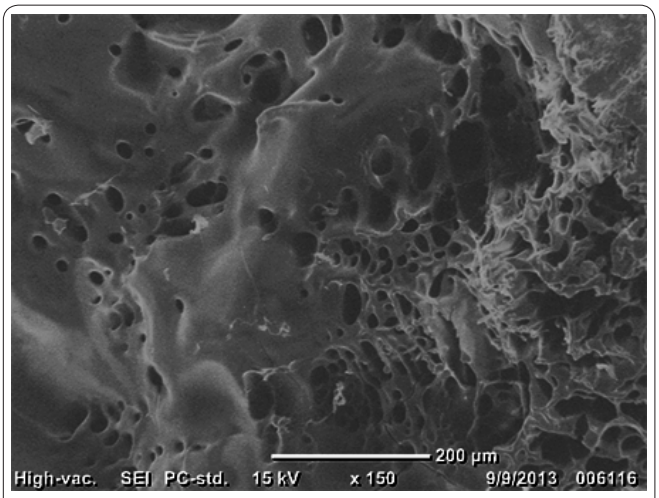

Figure 1. SEM image obtained from the ELT–PVP hydrogel. The image was recorded with a magnification of 150X, and the scale of the measuring bar is equivalent to 200 µm.

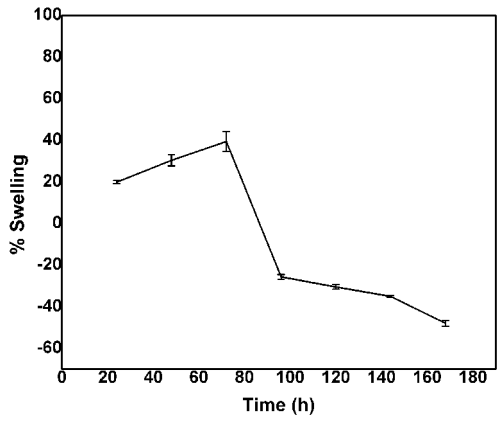

Figure 2. Percentage of swelling of the ELT–PVP hydrogel in PBS 1X at room temperature.

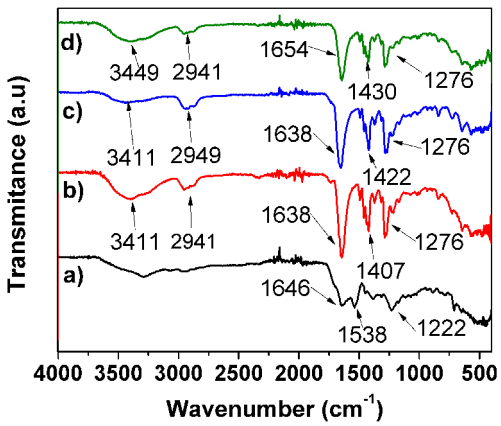

Figure 3. FTIR spectra of a) ELT, b) PVP, c) ELT+PVP, and d) ELT–PVP, respectively.

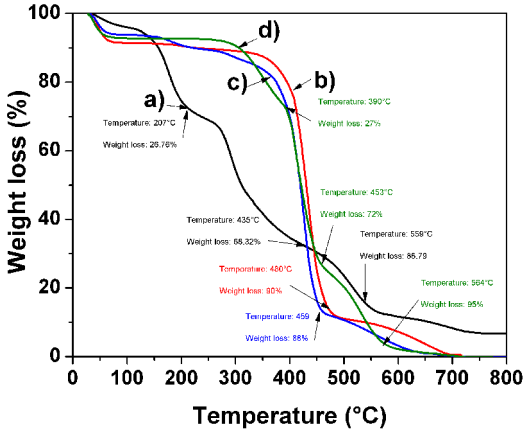

Figure 4. Thermograms obtained by TGA of a) ELT, b) PVP, c) ELT+PVP, and d) ELT–PVP, respectively.

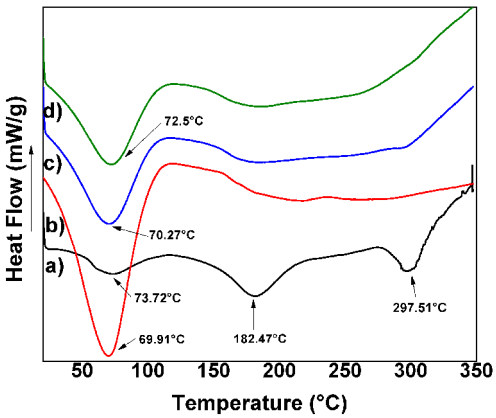

Figure 5. Thermograms obtained by DSC of a) ELT, b) PVP, c) ELT+PVP, and d) ELT–PVP, respectively.

observed at 1,538 cm^{-1} and 1,222 cm^{-1} were attributed to amide II and amide III, respectively. These types of signals are commonly presented in proteins spectra (17,18). For the PVP spectrum (line b), the bands located at 1,646 cm^{-1}, 1,407 cm^{-1}, and 1,276 cm^{-1} corresponded to the absorption band of the carbonyl group, the stretching vibration of CH bond, and the CN stretching vibration, respectively. These vibrations are characteristic of PVP (19). A notable change in the main bands was noted due to the effect of the induction of gamma radiation in ELT–PVP compared to ELT+PVP.

Thermal properties

In order to evaluate the thermal properties of the hydrogel, TGA, and DSC techniques were carried out. The thermograms obtained by TGA are depicted in Figure 4. The ELT–PVP profile exhibited a significant change in mass loss compared to the ELT+PVP profile, indicating structural changes in the formation of the new polymer.

The thermograms obtained by DSC analysis are shown in Figure 5, whereas the temperature and fusion enthalpy values obtained are presented in Table 1. The shift to the right of the melting peak of ELT–PVP compared to ELT+PVP represented additional evidence of the generation of cross-linking for the formation of ELT–PVP induced by gamma radiation.

Table 1. Fusion enthalpy values obtained in the DSC analysis.

	Temperature °C	ΔH (J/g)
ELT	73.72	52.3 ± 1.2
	182.47	171.6 ± 1.6
	297.51	113.2 ± 2.4
PVP K30	69.91	296.4 ± 2.2
ELT+PVP	70.27	637.7 ± 6.2
ELT–PVP	72.51	760.4 ± 11.5

Rheology

A rheological study was carried out to determine the fluidic properties of the ELT–PVP hydrogel and the ELT+PVP mixture to demonstrate the changes induced by gamma radiation in obtaining the novel hydrogel. The types of fluids are shown in Figure 6.

Cell viability assay

In order to evaluate the hydrogel biocompatibility, a cell viability test was carried out in human fibroblasts. The novel ELT–PVP hydrogel offered an increase in cell viability from a concentration of 0.15% compared to ELT alone (Figure 7).

Cell proliferation assay

The novel ELT–PVP hydrogel exhibited a considerable effect on cell proliferation from day three at a concentration of 0.15% (Figure 8), revealing a higher degree of protection compared to ELT than from day two at a concentration of 0.10, a significant change is exhibited.

Stability of ELT–PVP in cell culture medium

The biological characterization presented in Figure 9 illustrates the hydrogel's properties when exposed to the cell culture medium. Periodic evaluation of the hydrogel for seven days revealed a gradual decrease in the material's size due to its erosion.

Discussion

Morphology of the ELT–PVP hydrogel

The porosity and the presence of interconnected porous in biomaterials play a crucial role in cell mi-

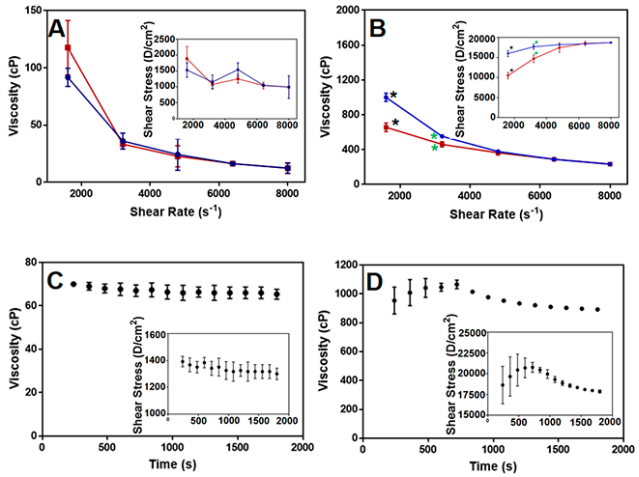

Figure 6. Rheological profile. (a) Variation of viscosity and shear stress with the applied shear rate for ELT+PVP, (b) variation of viscosity and shear stress with the applied shear rate for ELT–PVP, (c) Variation of viscosity across time with a constant shear rate for ELT+PVP, and (d) variation of viscosity across time with a constant shear rate for ELT–PVP. The blue curves correspond to the analysis increasing the shear rate, and the red curves correspond to the analysis decreasing the shear rate. Data are means ± SD of N = 3, * indicates a statistically significant difference at a 95% confidence level.

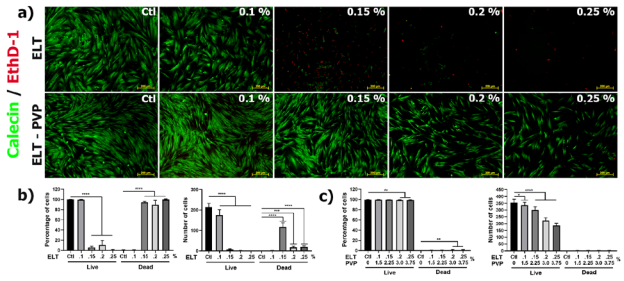

Figure 7. The blend of ELT and PVP improved cell viability in comparison with ELT alone. a) the photographs revealed the live cells in green (calcein positives) and dead cells in red (EthD-1 positives) with the different experimental conditions. In the bottom are exhibited the graphs of b) percentage and the number of cells in ELT and c) percentage and the number of cells of ELT–PVP hydrogels. ANOVA test, ***p =0.0001, ****p =0.00001.

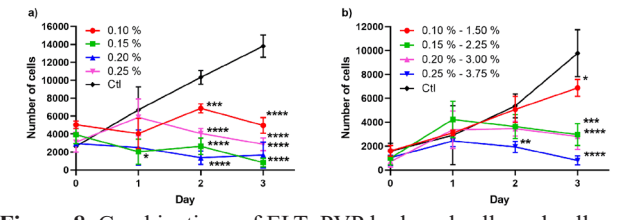

Figure 8. Combinations of ELT–PVP hydrogels allowed cell proliferation. The graph a) shows the proliferation curves of ELT and b) shows the proliferation curves of ELT–PVP. The ELT graphs show that the 0.10% treatment allows cell culture proliferation, while the ELT–PVP combination promotes proliferation until day 3, with a significance of ***p<0.0005 for the treatment of 0.10 and of *p<0.05 for the next two treatments (0.15 and 0.20).

gration and proliferation, especially in skin applications. The presence of porous can also facilitate the arrival of nutrients and oxygen to the cells because they allow the regeneration of blood vessels through angiogenesis and the development of new

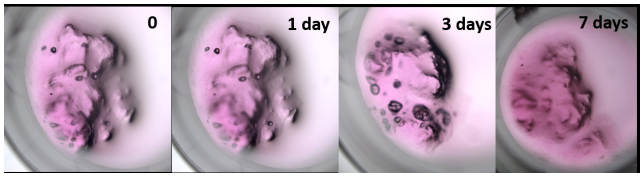

Figure 9. Stability assay of ELT–PVP hydrogel in cell culture condition at different times.

tissue (20). In this regard, Rnjak-Kovacina et al. (21) produced synthetic human ELT scaffolds with pore sizes between 8 and 11 µm, which permitted the infusion and proliferation of dermal fibroblasts on the scaffold surface. Similarly, another study found that ELT hydrogels presenting pores with an average size of around 15 µm were suitable for diffusing nutrients and oxygen (22). On the other side, it has been reported that pore size for cell infiltration of dermal fibroblasts in an ELT scaffold is 11 µm, whereas, for skin regeneration, the adequate size is 20 µm (22,23). Besides, the materials that present high porosity are enabled to the significant release of factors such as protein, genes, or cells, serving as platforms to administer bioactive substances in the wound bed (24). Therefore, the pores in the ELT–PVP hydrogel possesses an appropriate size for a wound dressing.

Swelling

The presence of the pores facilitates the entry of water into the hydrogel, promoting the relaxation of the polymer chains. Additionally, the carboxyl groups of ELT and the carbonyl groups of PVP favor the formation of hydrogen bonds for the uptake of water. The swelling process reaches a maximum at 72 h, and subsequently, a dissolution process was observed with subsequent weight loss. The swelling process could favor cell migration as a tissue scaffold, and it could even act as a possible wound dressing in wound healing processes by capturing exudate from the wound.

Spectral analysis

The ELT+PVP and ELT–PVP spectra indicated the characteristic bands presented in the PVP spectrum (lines c and d). This behavior could be related to that the PVP concentration is higher than the ELT concentration (15:1); thus, the PVP signals predominate. However, a slight decrease in the intensity of the bands was detected in the ELT–PVP spectrum. This decrement could be due to the radicals generated during the ELT–PVP cross-linking, inducing the homolytic cleavage of the C-H and CO-H bonds (25), which suggests that their concentrations in the medium are decreased.

ELT and PVP cross-linking reaction mechanism

The semi-solid ELT–PVP hydrogel presented a remarkable change in physical appearance compared with the un-irradiated liquid mixture. In this regard, due to the cross-linking of the polymer chains, changes in the physicochemical and biochemical properties of the copolymer are expected. It has been reported that radiation at 25 kGy is widely used to sterilize several types of materials

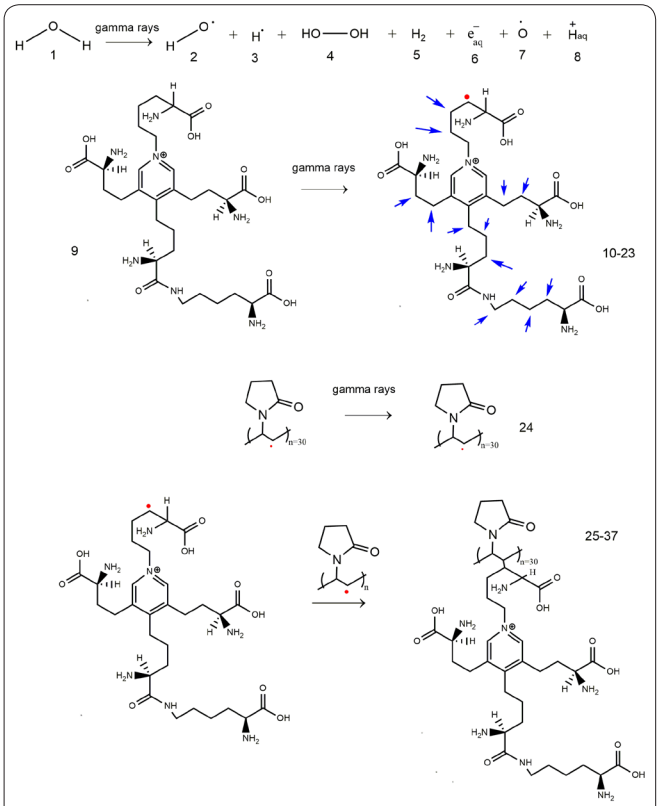

Figure 10. Proposed mechanism for synthesis of ELT–PVP hydrogel induced by gamma-radiation (see text for details).

and synthesize biomaterials applied in orthopedic, dental, and pharmaceutical fields (26). Furthermore, it has been reported that gamma radiation is an effective method to obtain protein-based hydrogels. For example, Chen et al. (27) developed a chitosan copolymer by this technique; the obtained scaffold presented a porous morphology, suitable mechanical properties, and high biocompatibility. Likewise, hydrogels of fibroin obtained through cross-linking showed excellent elastic properties, good compatibility, and biodegradability (28). Furthermore, PVP has been cross-linked with structural proteins, such as collagen, obtaining superabsorbent hydrogels (29). These characteristics allow the application of ELT- or PVP-based hydrogels in different fields, such as in cartilage engineering, vascular and skin grafts, among others (30).

Figure 10 presents the proposed mechanism for the synthesis of the ELT–PVP hydrogel by the simultaneous irradiation method. First, ELT and PVP are irradiated in the presence of water, under air conditions. Subsequently, the reacting mechanism could occur as follows: a) first, the irradiation step implies the formation of primary radicals; b) second, the initiation step provides the graft chain radicals; and finally, c) termination reactions are performed to yield the ELT–PVP hydrogel (31). The irradiation step includes the radiolysis of water (see compounds 2−8) (32), while different radicals of ELT (compounds 10−23) and PVP (compound 24) are formed (initiation step). Arrows depict the sites where ELT macroradicals can be developed. The termination reaction involves the deactivation of the ELT macroradicals with PVP radicals to yield the ELT–PVP hydrogel (compounds 25-37). Moreover, the complexity of the reaction also includes the possible formation of peroxides and hydroperoxides during the irradiation process (33). However, the decrease in the 3,400 cm^{-1} bands in FT-IR (Fig. 2) suggests that peroxides do not predominate, as compared to the graft reactions, to yield the hydrogel.

Thermal properties

According to TGA results (Figure 4), three significant weight losses were observed in the case of ELT (line a). The first one occurred from 100 to 207 °C, with a weight loss of 26.76%; this behavior is related to both the evaporation of water and the destabilization of non-covalent interactions, which do not require a large amount of energy. The second loss began at 205 °C and finished at 435 °C, with a total weight loss of 68.32%; in this range, the major denaturation transition occurs, triggering the ELT decomposition (34). The last thermic event was located from 450 to 559 °C, representing a total loss of 86.79%. For PVP analysis (Figure 4, line b), it could be observed the decomposition in a single stage from 375 to 449 °C, with a weight loss of approximately 95%; this deportment coincided with previous reports (35). For ELT+PVP (line c), the maximum decomposition temperature was 458 °C (similar to the PVP), and the weight loss was 88%; this behavior could be attributed to the proportion of PVP concerning the ELT. Finally, the biopolymer ELT–PVP (line d) presented some changes for its components. Three steps of weight loss were observed: the first one occurred between 320 and 390 °C, with 27% weight loss; the second one was found from 410 to 453 °C, losing 72% of the sample; finally, the third event was observed from 490 to 564 °C, showing a 95% of weight loss. The different events can be due to the decomposition of the three-dimensional structure, which changes from a complex three-dimensional network, stabilized by bridges of hydrogen or other weak interactions, to a more straightforward structure, where the covalent bonds predominate, increasing the required time and energy to decompose the molecule (36).

Concerning the DSC study (Figure 5, Table 1), previous studies showed that ELT presents an endothermic event at approximately 85 °C with an enthalpy of 191 J/g, which is attributed to the interaction between water and proteins, in addition to a second thermal transition at 200 °C (37). On the other hand, only one endothermic event was shown for the PVP at 69.91 °C (curve b), obtaining an enthalpy of fusion of 231 J /g. This value could be related to that PVP is a very hygroscopic material, so the steam from water can affect the calorific capacity. In the literature, this endothermic peak has been reported at around 100 °C and is attributed to the presence of water (38). The comparison between thermograms c) and d) let it observe a slight shift to the right, indicating the formation of new bonds.

Rheology

In order to determine the differences in the types of fluid between ELT+PVP mixture and ELT–PVP hydrogel (after the cross-linking of polymers), a rheological study was carried out. The shear rate test permitted to conclude that the hydrogel is a non-Newtonian fluid because the viscosity varied with the shear rate and time. Additionally, accord-

ing to the rheological profiles (Figure 6b), the hydrogel sample is similar to a pseudoplastic fluid with thixotropic behavior. In this regard, in pseudoplastic fluids, decrement in viscosity concerning shear rate is mainly due to the deconstruction of microstructures, allowing easy flow of the material. The reduction of hydrodynamic forces between the fluid and the microstructures cause this response, in addition to the alignment and deformation of these by the action of inertial forces (39). It is noteworthy that pseudo-plasticity is a suitable characteristic in topical products because it ensures uniform distribution of biopolymers on the skin. Likewise, thixotropy is another desired property, since it increases the retention time of the biopolymeric material at the topical application site. Moreover, pseudoplastic and thixotropic behavior can influence the bioadhesion properties of the dressing. Bioadhesion is pivotal because products intended to be in contact with the skin for prolonged periods will be subject to various stresses due to daily activities; thus, it must be ensured that the scaffold remains at the wound site (40–42).

Besides, when Figure 6a and Figure 6b were compared, the irradiated sample (Figure 6a) had viscosity values approximately 10-fold higher than the physical mixture (from 1,600 to 8,000 s^{-1}). This finding could be attributed to the cross-linking of the polymeric chains of ELT and PVP, which forms a three-dimensional network, increasing the molecular weight and the viscosity (43).

On the other hand, in the physical mixture (Figure 6a), a hysteresis cycle was not observed. However, at 1600s^{-1} and 4800 $s^{-1,}$ there was a separation of two points where there was no statistically significant difference between them. Contrariwise, in the ELT–PVP hydrogel (Figure 6b), a hysteresis loop, characteristic of thixotropic materials, was observed at 6,399.98 s^{-1} (44). In fluids with thixotropic behavior, the increase in velocity gradient (blue curve) causes the deconstruction of the structure, while the decrease in gradient (red curve) favors the reorganization (45). In the test of viscosity for the time at a constant shear rate, the physical mixture (Figure 6c) reached its maximum value at 240 s; after that, it presented a similar behavior to a Newtonian fluid (44). Whereas for the hydrogel (Figure 6d), an increase in viscosity is observed as time progresses, reaching a maximum value at approximately 720 s; after this point, it was found a decrement in viscosity toward constant values due to its thixotropic behavior.

Cell viability assay

Since ELT is an extracellular matrix protein, it was expected that the protein-maintained cell viability; however, surprisingly, only 0.1% w/v of ELT showed a high percentage of cell viability (99.4%); whereas higher concentrations of ELT (0.15, 0.2 and 0.25% w/v) revealed low values of viability (Figure 7a-7b). This finding could be explained by the presence of excessive ELT peptides that could produce an agonist effect in the ELT-laminin receptor. It should be considered that this receptor is dose-dependent; thus, the presence of saturating concentrations of ELT peptides results in chronic overstimulation of the receptor, which leads to sustained production of free radicals and lytic enzymes (46). Likewise, Fulop et al. (47) explained that leukocytes and endothelial cells, which activate the ELT-laminin receptor, trigger the release of nitric oxide and superoxide anion. The combination of both radicals forms the peroxynitrite anion, which is highly toxic. Besides, it has been demonstrated that at high concentrations of ELT, cell proliferation decreases (48).

Interestingly, the adverse effect of ELT was mitigated when it was combined with PVP. In all concentrations of ELT–PVP, the percentage of cell viability was high, although the number of cells decreased when the concentration of ELT and PVP increased (Figure 7c). In this respect, it has been reported that hydrogels combining PVP with other polymers by gamma irradiation do not possess cytotoxic effects (49). Therefore, this result suggests that combining ELT with PVP is an appropriate strategy for the biological applications of ELT because it improves its biocompatibility.

Cell proliferation assay

Similar to the viability test, cell proliferation assays demonstrated that only the concentration of 0.10% w/v of ELT allowed cell culture to proliferate. In contrast, higher concentrations (0.10, 0.15, and 0.20% w/v) of ELT–PVP allowed cell culture progression during the analysis time (3 days). In the proliferation assay may be understandable that high concentrations of ELT do not induce cell proliferation since the percentage of death is high in this condition. However, when fibroblasts were brought into contact with the ELT–PVP combination, they were able to proliferate. Concerning this, it has been established that the PVP of 40 and 360 kDa with a fractional volume occupancy (FVO; the volume occupied by macromolecules) between 18 and 54% may serve as a macromolecular crowder, allowing cell viability, proliferation, and the synthesis of extracellular matrix proteins. Noteworthy, this seems to be linked to the cell line employed, since these characteristics are enhanced more in human dermal fibroblasts than in bone marrow mesenchymal stem cells (50).

Stability of ELT–PVP in cell culture medium

The stability of ELT–PVP based on its appearance was analyzed by microscopy, and the obtained images are presented in Figure 9. After 24 h of the test, the hydrogel exposed the same morphology that the control. In the same way, on the third day of the experiment, the ELT–PVP presented a similar morphology after three days in culture conditions. At seven days, a slight degradation of the hydrogel could be observed. However, the integrity of the hydrogel structure remains in 80% approximately. This behavior demonstrated that the new copolymer is strong and suggests that its application as wound dressing could be adequate, allowing cell proliferation.

In this work, a novel ELT–PVP hydrogel was obtained through gamma irradiation of ELT and PVP in aqueous solution. The ELT–PVP hydrogel showed an ideal morphology to be used as scaffolding in wound healing because it allows cell migration and proliferation. Also, its high porosity could allow the significant

release of biologically active substances such as growth factors, genes, or drugs. Likewise, the rheological analysis evidenced that the new biopolymer exhibits a pseudoplastic fluid with thixotropic behavior, which confirms gamma radiation-induced changes in the chemical structure of the polymers. This property is useful since by applying a shear force on the hydrogel, it can flow and be applied easily into the wound, forming a protective film. Finally, the hydrogel exhibited a significantly higher percentage of cell viability concerning ELT, suggesting that the cross-linking of ELT with PVP is a suitable strategy for the biological applications of ELT to preserve the protein and ensure practical therapeutic applications.

Acknowledgments
This research was funded by CONACYT A1-S-15759 to Gerardo Leyva-Gómez. The authors would like to thank Miguel Ángel Canseco-Martínez for his help in providing the FTIR analysis, and Karla Eriseth Reyes-Morales for her technical assistance with thermal tests. The authors would like to thank to Elba Carrasco Ramírez, Irma Elena López Martínez and Ivonne Grisel Sánchez Cervantes from the Microscopy Core Facility from the School of Medicine at the UNAM for their technical assistance with microscopy assessment.

Conflicts of interest
There are no conflicts to declare.

Author contributions
Conceptualization, G.L.-G.; methodology, F.J.G.-Z., M.P.-D., and M.L.D.P.-A.; validation, R.S.-S., M.G.-T; formal analysis, F.J.G.-Z., M.L.D.P.-A., M.G.-T, G.F.-G, O.D.R.-H, M.G.-D.C., and G.L.-G.; investigation, F.J.G.-Z., and G.L.-G.; resources, M.L.D.P.-A., and G.L.-G.; data curation, F.J.G.-Z., M.L.D.P.-A., M.G.-T, and G.L.-G.; writing—original draft preparation, F.J.G.-Z., M.L.D.P.-A., and G.L.-G.; writing—review and editing, F.J.G.-Z., M.L.D.P.-A., M.G.-T, H.C., and G.L.-G.; visualization, G.L.-G.; supervision, M.L.D.P.-A., H.C., and G.L.-G.; project administration, M.L.D.P.-A. and G.L.-G.; funding acquisition, G.L.-G.

References

1. Morgado PI, Aguiar-Ricardo A, Correia IJ. Asymmetric membranes as ideal wound dressings: An overview on production methods, structure, properties and performance relationship. J Memb Sci [Internet]. 2015;490:139–51. Available from: http://dx.doi.org/10.1016/j.memsci.2015.04.064

2. Kokabi M, Sirousazar M, Hassan ZM. PVA-clay nanocomposite hydrogels for wound dressing. Eur Polym J. 2007;43(3):773–81.

3. Cortes H, Caballero-Florán IH, Mendoza-Muñoz N, Córdova-Villanueva EN, Escutia-Guadarrama L, Figueroa-González G, et al. Hyaluronic acid in wound dressings. Cell Mol Biol [Internet]. 2020 Jun 25;66(4):191. Available from: https://www.cellmolbiol.org/index.php/CMB/article/view/3722

4. Cortes, H., Caballero-Florán, I.H., Mendoza-Muñoz, N., Escutia-Guadarrama, L., Figueroa-González, G., Reyes-Hernández, O.D., González-Del Carmen, M., Varela-Cardoso, M., González-Torres, M., Florán, B., Del Prado-Audelo, M.L., Leyva-Gómez, G.Cortes, H., C G. Xanthan gum in drug release. Cell Mol Biol (Noisy-le-grand). 2020;66(5):199–207.

5. Guadarrama-Acevedo MC, Mendoza-Flores RA, Del Prado-Audelo ML, Urbán-Morlán Z, Giraldo-Gomez DM, Magaña JJ, et al. Development and Evaluation of Alginate Membranes with Curcumin-Loaded Nanoparticles for Potential Wound-Healing Applications. Pharmaceutics. 2019 Aug;11(8):1–20.

6. Gunatillake PA, Adhikari R, Gadegaard N. Biodegradable synthetic polymers for tissue engineering. Eur Cells Mater. 2003;5:1–16.

7. M I, El S, Magdi H Y. Hydrogel scaffolds for tissue engineering: Progress and challenges, Global Cardiology Science and Practice. A Qatar Found Acad J. 2015;44(April):317–42.

8. Kamoun EA, Kenawy ES, Chen X. A review on polymeric hydrogel membranes for wound dressing applications : PVA-based hydrogel dressings. J Adv Res. 2017;8:217–33.

9. Ochoa-Segundo EI, González-Torres M, Cabrera-Wrooman A, Sánchez-Sánchez R, Huerta-Martínez BM, Melgarejo-Ramírez Y, et al. Gamma radiation-induced grafting of n-hydroxyethyl acrylamide onto poly(3-hydroxybutyrate): A companion study on its polyurethane scaffolds meant for potential skin tissue engineering applications. Mater Sci Eng C [Internet]. 2020 Nov;116:111176. Available from: https://linkinghub.elsevier.com/retrieve/pii/S0928493120317094

10.Rosiak JM, Ulański P. Synthesis of hydrogels by irradiation of polymers in aqueous solution. Radiat Phys Chem. 1999;55(2):139–51.

11.Del Prado Audelo ML, Mendoza-Muñoz N, Escutia-Guadarrama L, Giraldo-Gomez D, González-Torres M, Florán B, et al. RECENT ADVANCES IN ELASTIN-BASED BIOMATERIALS. J Pharm Pharm Sci [Internet]. 2020 Aug 17;23:314–32. Available from: https://journals.library.ualberta.ca/jpps/index.php/JPPS/article/view/31254

12.Mithieux SM, Weiss AS. Elastin is a key extracellular matrix protein that is critical to the elasticity I . Elastic Fiber The extracellular matrix imparts structural integrity on the tissues and. Adv Portein Chem. 2006;70(04):437–61.

13.Almine JF, Wise SG, Weiss AS. Elastin signaling in wound repair. Birth Defects Res Part C - Embryo Today Rev. 2012;96(3):248–57.

14.Almine JF, Bax D V., Mithieux SM, Nivison-Smith L, Rnjak J, Waterhouse A, et al. Elastin-based materials. Chem Soc Rev. 2010;39(9):3371–9.

15.Jiang F, Wang X, He C, Saricilar S, Wang H. Mechanical properties of tough hydrogels synthesized with a facile simultaneous radiation polymerization and cross-linking method. Radiat Phys Chem. 2015;106:7–15.

16.Leyva-Gómez G, Lima E, Krötzsch G, Pacheco-Marín R, Rodríguez-Fuentes N, Quintanar-Guerrero D, et al. Physicochemical and functional characterization of the collagen- polyvinylpyrrolidone copolymer. J Phys Chem B. 2014;118(31):9272–83.

17.Baker MJ, Trevisan J, Bassan P, Bhargava R, Butler HJ, Dorling KM, et al. Using Fourier transform IR spectroscopy to analyze biological materials. Nat Protoc. 2014;9(8):1771–91.

18.Riaz T, Zeeshan R, Zarif F, Ilyas K, Muhammad N, Safi SZ, et al. FTIR analysis of natural and synthetic collagen. Appl Spectrosc Rev. 2018;53(9):703–46.

19.González-Torres M, Leyva-Gómez G, Rivera M, Krötzsch E, Rodríguez-Talavera R, Rivera AL, et al. Biological activity of radiation-induced collagen–polyvinylpyrrolidone–PEG hydrogels. Mater Lett. 2018;214:224–7.

20.Loh QL, Choong C. Three-dimensional scaffolds for tissue engineering applications: role of porosity and pore size. Tissue Eng Part B Rev. 2013;19(6):485–502.

21.Rnjak-Kovacina J, Wise SG, Li Z, Maitz PKM, Young CJ, Wang Y, et al. Tailoring the porosity and pore size of electrospun synthetic human elastin scaffolds for dermal tissue engineering. Biomaterials.

2011;32(28):6729–36.
22.Annabi N, Mithieux SM, Weiss AS, Dehghani F. The fabrication of elastin-based hydrogels using high pressure CO2. Biomaterials. 2009;30(1):1–7.
23.Yannas I V, Lee E, Orgill DP, Skrabut EM. Synthesis and characterization of a model extracellular matrix that induces partial regeneration of adult mammalian skin. Proc Natl Acad Sci. 1989;86(February):933–7.
24.Hollister SJ. Porous scaffold design for tissue engineering. Nat Mater. 2005;4(July):518–24.
25.Atrous H, Benbettaieb N, Hosni F, Danthine S, Blecker C, Attia H, et al. Effect of γ-radiation on free radicals formation, structural changes and functional properties of wheat starch. Int J Biol Macromol. 2015;80:64–76.
26.Benson RS. Use of radiation in biomaterials science. Nucl Instruments Methods Phys Res Sect B Beam Interact with Mater Atoms. 2002;191(1–4):752–7.
27.Chen Z, Du T, Tang X, Liu C, Li R, Xu C, et al. Comparison of the properties of collagen–chitosan scaffolds after γ-ray irradiation and carbodiimide cross-linking. J Biomater Sci Polym Ed. 2016;27(10):937–53.
28.Kim MH, Park WH. Chemically cross-linked silk fibroin hydrogel with enhanced elastic properties, Biodegradability, and biocompatibility. Int J Nanomedicine. 2016;11:2967–78.
29.Demeter M, Virgolici M, Vancea C, Scarisoreanu A, Kaya MGA, Meltzer V. Network structure studies on γ–irradiated collagen–PVP superabsorbent hydrogels. Radiat Phys Chem. 2017;131:51–9.
30.Nettles DL, Chilkoti A, Setton LA. Applications of elastin-like polypeptides in tissue engineering. Adv Drug Deliv Rev. 2010;62(15):1479–85.
31.Segura T, Menes-Arzate M, León F, Ortega A, Burillo G, Peralta RD. Synthesis of narrow molecular weight distribution polyvinyl acetate by gamma–rays initiated RAFT/MADIX miniemulsion polymerization. Polymer (Guildf). 2016;102:183–91.
32.González Torres M, Cerna Cortez J, Balam Muñoz Soto R, Ríos Perez A, Pfeiffer H, Leyva Gómez G, et al. Synthesis of gamma radiation-induced PEGylated cisplatin for cancer treatment. RSC Adv. 2018;8(60):34718–25.
33.Nimse SB, Pal D. Free radicals, natural antioxidants, and their reaction mechanisms. RSC Adv. 2015;5(35):27986–8006.
34.Bellissent-Funel MC, Hassanali A, Havenith M, Henchman R, Pohl P, Sterpone F, et al. Water Determines the Structure and Dynamics of Proteins. Chem Rev. 2016;116(13):7673–97.
35.Silva MF, Da Silva CA, Fogo FC, Pineda EAG, Hechenleitner AAW. Thermal and ftir study of polyvinylpyrrolidone/lignin blends. J Therm Anal Calorim. 2005;79(2):367–70.
36.Wang M, Duan X, Xu Y, Duan X. Functional Three-Dimensional Graphene/Polymer Composites. ASC Nano. 2016;
37.Samouillan V, Dandurand-Lods J, Lamure A, Maurel E, Lacabanne C, Gerosa G, et al. Thermal analysis characterization of aortic tissues for cardiac valve bioprostheses. J Biomed Mater Res. 1999;46(4):531–8.
38.Zhou R, Wang F, Chang M, Yue H, Shi L, Zhao Y. Preparation and evaluation of solid dispersion of asiatic acid with PVPk30. Dig J Nanomater Biostructures. 2012;7(3):1015–20.
39.Vaccaro A, Marrucci G. A model for the nonlinear rheology of associating polymers. J Nonnewton Fluid Mech. 2000;92(2–3):261–73.
40.Carvalho FC, Calixto G, Hatakeyama IN, Luz GM, Gremião MPD, Chorilli M. Rheological, mechanical, and bioadhesive behavior of hydrogels to optimize skin delivery systems. Drug Dev Ind Pharm. 2013;39(11):1750–7.
41.Lee CH, Moturi V, Lee Y. Thixotropic property in pharmaceutical formulations. J Control Release. 2009;136(2):88–98.
42.Martín MJ, Calpena AC, Fernández F, Mallandrich M, Gálvez P, Clares B. Development of alginate microspheres as nystatin carriers for oral mucosa drug delivery. Carbohydr Polym. 2015;117:140–9.
43.T.Shaw M. Introduction to polymer rheology. New Jersey: John Wiley and Sons, Inc; 2012. 335 p.
44. Osswald R. Polymer Rheology. Munich: HANSER; 2015. 7–10 p.
45.Dinkgreve M, Fazilati M, Denn MM, Bonn D. Carbopol: From a simple to a thixotropic yield stress fluid. J Rheol (N Y N Y). 2018;62(3):773–80.
46.Larbi A, Levesque G, Robert L, Gagné D, Douziech N, Fülöp T. Presence and active synthesis of the 67 kDa elastin-receptor in human circulating white blood cells. Biochem Biophys Res Commun. 2005;332(3):787–92.
47.Fulop T, Larbi A, Fortun A, Robert L, Khalil A. Elastin peptides induced oxidation of LDL by phagocytic cells. Pathol Biol. 2005;53(7):416–23.
48.Péterszegi G, Texier S, Robert L. Cell death by overload of the elastin-laminin receptor on human activated lymphocytes: Protection by lactose and melibiose. Eur J Clin Invest. 1999;29(2):166–72.
49.Lugão AB, Rogero SO, Malmonge SM. Rheological behaviour of irradiated wound dressing poly(vinyl pyrrolidone) hydrogels. Radiat Phys Chem. 2002;63(3–6):543–6.
50.Rashid R, Lim NSJ, Chee SML, Png SN, Wohland T, Raghunath M. Novel use for polyvinylpyrrolidone as a macromolecular crowder for enhanced extracellular matrix deposition and cell proliferation. Tissue Eng - Part C Methods. 2014;20(12):994–1002.